



OPEN

Characteristics of heavy metal element content and health risk assessment in groundwater in Zhaojue area, Sichuan Province, China

Yongsheng Lin^{1,2,3}✉, Jinhui Liu¹, Shengzhang Zou^{2,3}, Jia Wang^{2,3}, Lianjie Fan^{2,3}, Changsong Zhou^{2,3} & Li Lu^{2,3}

Groundwater serves as the primary drinking water source for residents in the Zhaojue area, located in the hinterland of the Daliang Mountains in Sichuan Province. This study investigated the spatial distribution, pollution characteristics, and health risks of 10 metal elements (As, Cd, Al, Mn, Hg, Co, Cu, Pb, Zn, Ni) through 48 groundwater sampling sites. Comprehensive analysis using single-factor and Nemerow composite pollution index evaluation methods, coupled with multivariate statistics and health risk models, revealed critical findings. The mean concentrations followed the order: Al > Mn > As > Cu > Zn > Hg > Cd > Pb > Ni > Co, with 1 site exceeding Al standards and 3 sites surpassing Hg limits. Spatial analysis showed elevated metal concentrations in eastern and central regions compared to western areas. Source apportionment identified three primary origins: Zn-Ni-Pb from industrial/agricultural/transportation activities (44.8% contribution), Co-Cu-Mn-Al from geological sources (22.2%), and Hg-As-Cd from mixed natural-anthropogenic sources (10.5%). While Nemerow indices indicated generally good water quality (89.58% of samples unpolluted), the health risk assessment revealed that children exhibited higher non-carcinogenic risks (HI: 0.41–3.36) compared to adults (HI: 0.16–1.33), with forty-four child samples exceeding the safety threshold (HI > 1). All child samples surpassed the incremental lifetime cancer risk (ILCR) threshold (1.0×10^{-4}), whereas only 20.8% of adult samples exceeded this limit. Arsenic was the main pollutant and ingestion was the main exposure pathway. These findings underscore significant carcinogenic risks in the studied area, necessitating urgent groundwater management interventions to mitigate health threats, particularly for vulnerable children.

Keywords Groundwater metal contamination, Health risk assessment, Source apportionment, Drinking water safety

Groundwater constitutes a critical component of global water resources, representing approximately 99% of Earth's liquid freshwater reserves. This vital resource plays an indispensable role in supporting drinking water supplies, agricultural irrigation, industrial processes, and ecosystem maintenance. Notably, groundwater serves as the primary domestic water source for nearly half of the global population¹. The emergence of heavy metal contamination in groundwater systems has become a pressing global environmental concern. These pollutants exhibit particular environmental persistence and bioaccumulative potential, with even trace concentrations capable of inducing irreversible damage to human health and ecological systems². The International Agency for Research on Cancer (IARC) classifies cadmium as a Group 1 human carcinogen. Chronic exposure to cadmium-contaminated groundwater has been epidemiologically associated with elevated risks of multiple malignancies, including pulmonary carcinoma, prostatic neoplasms, and mammary gland tumors^{3,4}. Mercury

¹School of Water Resources and Environmental Engineering, East China University of Technology, Nanchang 330000, China. ²Institute of Karst Geology, CAGS/Key Laboratory of Karst Dynamics, MNR & GZAR/International Research Centre on Karst under the Auspices of UNESCO, Guilin 541004, Guangxi, China. ³Pingguo Guangxi, Karst Ecosystem, National Observation and Research Station, Pingguo 531406, Guangxi, China. ✉email: 516256973@qq.com

compounds demonstrate multi-pathway exposure routes through contaminated water sources, with chronic exposure potentially inducing toxicological impacts across multiple organ systems encompassing dermatological manifestations, cardiovascular dysfunction, respiratory compromise, renal impairment, gastrointestinal disturbances, and neurotoxic sequelae⁵. Long-term exposure to arsenic, for instance, can lead to serious health risks, including hypertension, skin lesions, neurodegenerative diseases, cancer, and cardiovascular diseases^{6,7}. Furthermore, high concentrations of copper, iron, manganese, and zinc may also pose health risks, such as excessive zinc levels increasing the risk of intestinal toxicity⁸. Therefore, it is imperative to study the content and distribution of heavy metals in water environments and their impacts on human health.

In recent years, single-factor evaluation methods and the Nemerow index method have gained widespread adoption in groundwater quality assessments both domestically and internationally, primarily due to their capacity to directly quantify pollutant concentration exceedances^{9,10}. Principal component analysis (PCA) has primarily been applied to groundwater source apportionment^{11,12}. However, reliance solely on water quality assessment outcomes may prove inadequate for water safety decision-making, potentially underestimating health risks posed by heavy metal elements that remain below regulatory thresholds. The health risk assessment model established by the U.S. Environmental Protection Agency (US EPA) provides a robust framework for evaluating groundwater-related health risks, with typical exposure pathways including drinking water ingestion and dermal contact. Substantial epidemiological evidence confirms that chronic exposure to heavy metals via these routes can induce significant direct and indirect health consequences^{13,14}.

Zhaojue area is located in the hinterland of the Daliang Mountains and was once a deeply impoverished county in the Wumeng Mountains. Formerly designated as a national poverty-stricken county, this region has been prioritized among 150 key counties for state-supported rural development programs. Since the early 21st century, particularly following the implementation of targeted poverty alleviation strategies in 2013, extensive geological investigations have been conducted by the China Geological Survey to support sustainable development in this ecologically sensitive area¹⁵. Cao Jun et al.¹⁶ studied the geochemical characteristics of Emeishan basalt in Zhaojue area, indicating that basalt has obvious high SiO_2 , Fe_2O_3 , and TiO_2 characteristics; Zhou Changsong et al.¹⁷ found that the H_2SiO_3 -rich groundwater in Zhaojue area is mainly distributed in basalt areas, and proposed to develop metasilicate mineral water; Fan Lianjie et al.¹⁸ summarized three groundwater development and utilization models in Zhaojue County, providing a basis for solving the water shortage in the area. Lu Li et al.¹⁹ analyzed the hot spring water in Zhuhuo, Zhaojue, and found that the hot spring water is rich in various trace elements essential for human health, such as strontium and metasilicate. Lin et al.²⁰ evaluated the quality of groundwater in the northern part of Zhaojue area, and found that the overall quality is good. Notwithstanding, currently, there is a dearth of research on the environmental quality of groundwater in Zhaojue County, especially with respect to the environmental status of heavy metals in groundwater. This deficiency renders it challenging to meet the requirements for the development and utilization of safe drinking water in Zhaojue County. In this study, the Zhaojue area was selected as the research target. A total of 48 groups of groundwater samples were collected, and 10 heavy metals (As, Cd, Al, Mn, Hg, Co, Cu, Pb, Zn, and Ni) were detected. The spatial distribution characteristics of these heavy metals were analyzed using ArcGIS. The sources of heavy metals were identified through correlation coefficient analysis and principal component analysis. Water quality was evaluated by means of single - factor evaluation and the Nemerow comprehensive pollution index method. Finally, a human health risk assessment was carried out for both adults and children using a health risk assessment model, with the objective of providing a reference for groundwater environmental protection, as well as development and utilization in the Zhaojue area.

Materials and methods

Study area

Zhaojue County is situated in the east-central region of Liangshan Yi Autonomous Prefecture, Sichuan Province, within the upper reaches of the Xixi River, which is part of the Jinsha River basin. It is a typical “Yi - inhabited county” in China, spanning longitudes from 102°22'E to 103°19'E and latitudes from 27°45'N to 28°21'N, with an approximate area of 2697.63 km²²¹. The county's geological structure belongs to the Kangdian platform anticline east wing, which is strongly cut and eroded by the Jinsha River system, resulting in a lower erosion datum in the east and a high-west low-landform type. The county's terrain is divided into low mountains, low-middle mountains, middle mountains, mountain plains, intermountain basins, terraces and floodplains, alluvial fans, slope-deposited skirts, etc. The climate has characteristics of plateau climate, belonging to the Yalong River temperate climate zone in western Sichuan Plateau with an average annual temperature of 10.9°C and an average annual rainfall of 846.1 mm.

Zhaojue County is located in the north-south geological tectonic belt between Sichuan and Yunnan provinces. The western part of the county, on the eastern edge of the Mishi syncline, exposes strata mainly composed of relatively recent Cretaceous and Jurassic red clastic rocks, along with Quaternary sediments in the Saladi slope basin and Pushi area. In the central part of the county, four major faults (Puxiong River fault, Mufoshan fault, Rekou fault, and Zhune fault) are particularly well - developed. The exposed strata here mainly consist of Permian Emeishan basalt, limestone, Jurassic clastic rocks, Triassic limestone and clastic rocks, as well as Quaternary sediments in the Zhaojue Basin and Zhune Basin. The northern Bil - Yangmo rent area is mostly covered by exposed Jurassic clastic rocks. The eastern part of the county mainly exposes Permian basalt, Triassic limestone, and clastic rocks. Based on differences in formation lithology, rock associations, and water - bearing properties, the groundwater types in the study area can be classified into four categories: pore water in loose rocks, pore - fissure water in clastic rocks, fissure water in basalt, and fissure - cave water in carbonate rocks. The recharge, runoff, discharge conditions, and dynamic changes of groundwater are governed by factors such as climate, geomorphology, and tectonics. Groundwater in the study area is generally recharged by atmospheric precipitation. Due to the significant uplift of near - surface structures, steep valley slopes, and short runoff paths,

the runoff direction is constrained by lithological composition, structure, and geomorphology. Groundwater discharges in the form of springs in various major river systems, tributary valleys, and intermountain basins. Furthermore, in the carbonate-rock area, the terrain, which is steep and narrow due to fold development, and the widespread distribution of aquifers are not conducive to the infiltration of precipitation and surface water. As a result, surface karstification is underdeveloped, groundwater distribution is uneven, and outcrops are scarce. However, in monocline mountains and faults that have a wide - ranging influence on groundwater, it is mainly concentrated in the form of springs and underground rivers.

Groundwater sampling and analysis

In this study, a total of 48 groundwater samples were collected in Zhaojue County, and the location information of sampling points is shown in Fig. 1. During sample collection, the 500 mL polyethylene sampling bottle was cleaned three times with the original water, and the original water was filtered with a filter membrane with an aperture of 0.45 μm . 500 mL water samples were collected for each group of samples, and 1:1 nitric acid 2 mL was added to stabilize the metal elements in the filtered water sample. The bottle mouth was sealed with a sealing film. After sampling, the researchers record the surrounding environment, human activities, and possible sources of pollution. After collection, all water samples were put into an incubator for transportation and preservation, and quickly sent to the Karst Geology and Resource Environment Testing Center of the Ministry of Natural Resources for testing related components.

The concentrations of heavy metals (As, Cd, Al, Mn, Hg, Co, Cu, Pb, Zn, and Ni) in all filtered and acidified water samples were determined using an inductively coupled plasma mass spectrometer (ICP-MS) under standard operating conditions. To ensure data quality, each sample was analyzed in triplicate and the average value was taken as the final concentration. Calibration blanks and independent calibration verification criteria were established for every 15 sample analyses. The standard deviations of all heavy metal elements were below 5%, and the recoveries ranged from 90 to 110%. Therefore, the results of metal detection in the water samples are reliable and suitable for further analysis.

Groundwater quality evaluation method

1. Single factor pollution index method.

The single factor evaluation method is used to indicate whether a single indicator of water quality has reached the specified water functional category or exceeded the standard, and to determine the main heavy metal pollutants^{22,23}. Moreover, it is one of the most commonly used methods for water quality evaluation both domestically and internationally²⁴. The single factor pollution index is the ratio of the measured value of the project to the evaluation standard value:

$$P_i = \frac{C_i}{B_i} \quad (1)$$

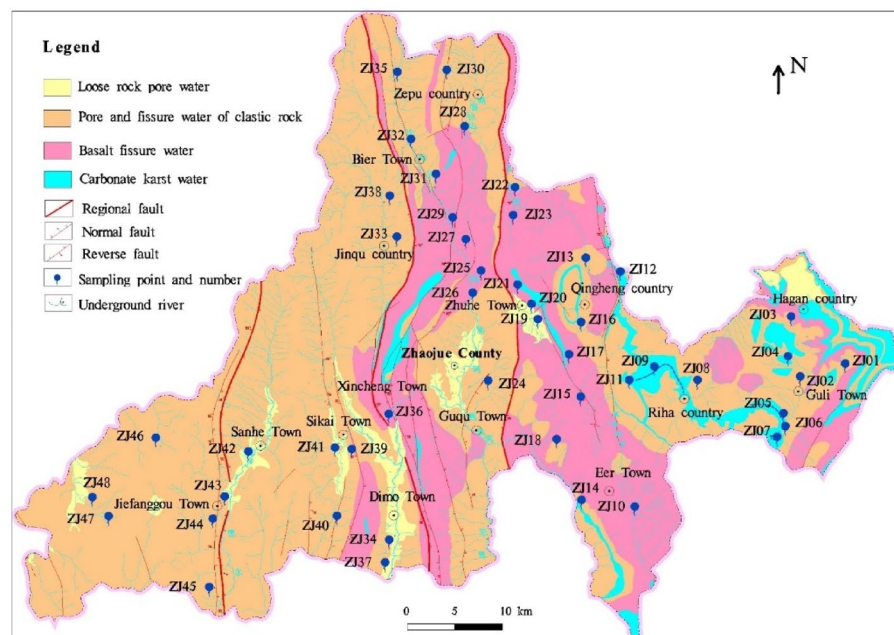


Fig. 1. Map of hydrogeological background and sampling point distribution in the research area.

In the formula(1), P_i represents the pollution index of single water quality index i ; C_i denotes the measured value of heavy metal element i ; and B_i stands for the standard limit value of heavy metal element according to Class III of the groundwater quality standard. Moreover, the evaluation grading standard for groundwater quality using the single factor pollution index method is presented in Table 1¹⁰.

2. Nemerow pollution index method.

The Nemerow comprehensive index evaluation method, built upon the single factor evaluation method, comprehensively takes into account the maximum and average values of the single factor pollution index and can accentuate heavy metal elements causing severe environmental pollution²⁵.

$$P_N = \sqrt{\frac{P_{imax}^2 + P_{iave}^2}{2}} \tag{2}$$

In the formula (2), P_N is the Nemerow comprehensive pollution index; P_{imax} is the maximum value of the single factor pollution index of heavy metal element i ; P_{iave} is the average of the single factor pollution index of heavy metal element i . The grading standard for environmental quality evaluation by the Nemerow pollution index method is shown in Table 1¹⁰.

3. Human Health Risk (HHR) Assessment.

Heavy metal elements in water bodies can introduce pollutants to the human body mainly through two exposure pathways: ingestion and dermal contact. These two pathways can bring more than 90% of pollutants to the human body^{26,27}. According to the reliability analysis of carcinogenic chemical substances detected by the World Health Organization (WHO) and the International Agency for Research on Cancer (IARC), metal elements can be divided into two categories: chemical carcinogenic metal elements and non chemical carcinogenic metal elements. In the groundwater of the study area, metal elements can also be divided into two groups: chemical carcinogenic heavy metal elements such as As and Cd, and non chemical carcinogenic heavy metal elements including Al, Cu, Pb, Zn, Ni, Co, Mn, and Hg. Using the health risk assessment model recommended by the US EPA for harmful substances in water environments^{28–31} health risk assessments were conducted for adults and children, respectively. First, chronic daily intake (CDI) for both exposure pathways was evaluated as follows:

$$CDI_{ing} = \frac{c_w \times IR \times EF \times ED}{BW \times AT} \tag{3}$$

$$CDI_{derm} = \frac{c_w \times SA \times Kp \times ET \times ED \times EF \times CF}{BW \times AT} \tag{4}$$

All exposure factors in Eqs. (4) and (5) are given in Tables 2 and 3^{32–36}. The hazard index (HI) was calculated to assess the non-carcinogenic risk. It is derived from the sum of the hazard quotient via ingestion (HQ_{ing}) and dermal exposure (HQ_{derm}) as follows:

$$HQ_{ing} = \frac{CDI_{ing}}{RfD_{ing}} \tag{5}$$

$$HQ_{derm} = \frac{CDI_{derm}}{RfD_{derm}} \tag{6}$$

$$HI = \sum (HQ_{ing} + HQ_{derm}) \tag{7}$$

Water quality level	Pi	Pollution assessment	PN	Pollution assessment
I	≤ 1	No pollution	<0.59	No pollution
II	(1,2]	Slightly pollution	[0.59,0.74)	Slightly pollution
III	(2,3]	Lightly pollution	[0.74,1.00)	Lightly pollution
IV	(3,5]	Moderately polluted	[1.00,3.50)	Moderately polluted
V	>5	Seriously pollution	≥ 3.50	Seriously pollution

Table 1. Evaluation criteria for the single-factor pollution index and the Nemerow pollution index.

HMs			SF/(kg d) mg ⁻¹		RfD/mg (kg d) ⁻¹		ED/a	AT/d
			Ingestion	Dermal contact	Ingestion	Dermal contact		
Carcinogenic	As	1	1.5	3.66	0.0003	0.000123	70	25,550
	Cd	1	6.1	6.1	0.001	0.00001		
	Pb	0.1	0.0085	–	0.0035	0.000525		
Non-carcinogenic	Al	1	–	–	0.14	14	35	12,775
	Cu	1	–	–	0.04	0.012		
	Zn	0.6	–	–	0.3	0.06		
	Ni	0.2	–	–	0.02	0.0054		
	Co	0.4	–	–	0.0003	0.0003		
	Mn	1	–	–	0.14	0.0018		
	Hg	1	–	–	0.0003	0.0003		

Table 2. Related parameter values of health risk assessment methods (carcinogenic and Non carcinogenic).

Parameter	Meaning	Value		Unit
		Adults	Children	
Cw	The concentration of heavy metals	Measured values	Measured values	mg L ⁻¹
IR	Ingestion rate	1.542	1	L d ⁻¹
EF	Exposure frequency	365	365	d a ⁻¹
BW	The average body weight	58.1	15.0	kg
SA	Surface area in contact with the skin	18,000	6000	cm ²
ET	Exposure time	0.6333	0.4167	h d ⁻¹
CF	Volume conversion factor	1	1	mL cm ⁻³

Table 3. Parameter values related to health risk assessment methods (adults and children).

where RfD_{ing} and RfD_{derm} represent the reference dose of each contaminant in (mg (kg d)⁻¹) via the ingestion and dermal exposure pathways, respectively (Table 2)^{37–39}. An HI value > 1 indicate unacceptable non-carcinogenic risk. In contrast, no risk is present. Carcinogenic risk is represented through the measure of incremental lifetime cancer risk (ILCR), which represents the sum of carcinogenic risk via ingestion (CR_{ing}) and dermal exposure (CR_{derm}), as follows:

$$CR_{ing} = CDI_{ing} \times SF_{ing} \tag{8}$$

$$CR_{derm} = CDI_{derm} \times SF_{derm} \tag{9}$$

$$ILCR = \sum (CR_{ing} + CR_{derm}) \tag{10}$$

where SF_{ing} and SF_{derm} represent the slope factors of carcinogenic contaminants for the ingestion and dermal exposure pathways, respectively (Table 2). According to the USEPA guidelines, $ILCR > 10^{-4}$, $10^{-6} < ILCR < 10^{-4}$, and $ILCR < 10^{-6}$ designate unacceptable, tolerable, and negligible carcinogenic risk, respectively.

Multivariate statistical analysis methods

The Pearson Correlation Coefficient can reflect the degree of linear correlation between two random variables. The value of the correlation coefficient r ranges from -1 to 1 . If $r > 0$, it indicates that the two variables are positively correlated; If $r < 0$, it indicates that the two variables are negatively correlated, and the larger the absolute value of r , the stronger the correlation; If $r = 0$, it indicates that there is no linear correlation between the two. Generally, it is considered that when the correlation coefficient is between 0 and 0.2 , the two variables are either uncorrelated or extremely weakly correlated; when it is between 0.2 and 0.4 , they are weakly correlated; when it is between 0.4 and 0.6 , they are moderately correlated; when it is between 0.6 and 0.8 , they are strongly correlated; and when it is between 0.8 and 1 , they are extremely strongly correlated^{40–42}. Principal component analysis is the process of transforming many relevant influencing indicators into a few main indicators through dimensionality reduction, and the extracted main indicators can retain most of the original information to ensure the reliability of the analysis results. It can be used to evaluate the spatial changes and sources of heavy metals in groundwater^{43–46}.

Results and discussion
Characteristics of heavy metal concentration

The concentrations of heavy metals in groundwater in the Zhaojue area are presented in Table 4, revealing significant variations among the concentrations of various heavy metals. The average concentrations of As, Cd, Al, Mn, Hg, Co, Cu, Pb, Zn, and Ni are 1.17, 0.22, 45.44, 6.43, 0.37, 0.10, 0.60, 0.17, 0.49, and 0.17 $\mu\text{g L}^{-1}$, respectively. All average concentrations of heavy metals fall below the Class III standards specified in the Standard for groundwater quality (GB/T 14848–2017) and the standards specified in the Standards for drinking water quality (GB 5749–2022). The concentration values are in the following order: $\text{Al} > \text{Mn} > \text{As} > \text{Cu} > \text{Zn} > \text{Hg} > \text{Cd} > \text{Pb} > \text{Ni} > \text{Co}$. Notably, aluminum exhibited the highest mean concentration (45.44 $\mu\text{g L}^{-1}$; range: 2.21–305.99 $\mu\text{g L}^{-1}$), with one sample exceeding the standard limit by 1.53-fold. Manganese showed a mean concentration of 6.42 $\mu\text{g L}^{-1}$ (range: 0.07–57.50 $\mu\text{g L}^{-1}$), where three sampling points surpassed regulatory limits, reaching up to 7.05 times the permissible level.

The coefficient of variation can reflect the degree of dispersion of element content in the sample, and the larger the coefficient of variation, the greater the degree of fluctuation. According to Stoeva et al.⁴⁷ the degree of variation can be classified as follows: $\text{CV} \leq 20\%$ is low variability, $20\% < \text{CV} \leq 50\%$ is moderate variability, and $50\% < \text{CV} \leq 100\%$ is high variability. In the groundwater of the study area, the coefficients of variation of As, Al, Mn, Hg, Co, Cu, Pb, Zn, and Ni all exceeded 50%, with Hg having the highest coefficient of variation at 321.43%. The high variability of these nine heavy metals and the significant differences in their coefficients of variation suggest that heavy metals in the study area are greatly influenced by the groundwater occurrence space, and the pollution sources and pathways of different heavy metals vary. In contrast, the coefficient of variation of Cd is the smallest, at 35.59%, indicating that the concentration distribution of Cd is relatively stable.

The average concentration of heavy metal elements in the study area is 55.16 $\mu\text{g L}^{-1}$. As shown by the accumulation of total concentration at each sampling point (Fig. 2), the concentration ranges from 2.82 to 311.12 $\mu\text{g L}^{-1}$. Metal elements detected in more than 50% of the samples include As, Cd, Al, Mn, Co, Cu, and Ni. Among them, As, Al, and Mn were detected in all samples (100%). The sampling site with the highest total - concentration accumulation value was ZJ13, with a concentration of 311.12 $\mu\text{g L}^{-1}$, while the lowest was ZJ33, with a concentration of 2.82 $\mu\text{g L}^{-1}$. The sites that contributed most to the average concentration were ZJ13, ZJ22, and ZJ38.

Spatial distribution characteristics of heavy metals

The spatial distribution characteristics of heavy metal concentrations in groundwater within the study area exhibit significant regional heterogeneity. Using the Inverse Distance Weighting (IDW) method⁴⁸, we mapped the spatial distribution of metal elements with detection rates exceeding 50% in groundwater samples from Zhaojue area (As, Al, Mn, Co, Cu, Ni, and Cd; Fig. 3). Notably, arsenic exhibited a distinct hotspot in southeastern Zhaojue, with the maximum concentration (5.18 $\mu\text{g L}^{-1}$) recorded at sampling site ZJ17. Aluminum distribution presented three discrete zones, peaking at 305.99 $\mu\text{g L}^{-1}$ in northeastern site ZJ13. Manganese concentrations formed three localized hotspots, reaching 57.50 $\mu\text{g L}^{-1}$ at northeastern site ZJ22. Cobalt distribution revealed dual high-concentration zones: a primary northeastern hotspot (0.71 $\mu\text{g L}^{-1}$ at ZJ22) and a secondary central zone (0.52 $\mu\text{g L}^{-1}$ at ZJ36). Copper displayed a northeast-southwest trending belt of elevated concentrations, peaking at 3.10 $\mu\text{g L}^{-1}$ in the northeastern sector (ZJ22). Nickel accumulation formed clustered high-concentration blocks in central and southern regions, attaining 3.10 $\mu\text{g L}^{-1}$ at central site ZJ36. In contrast, cadmium concentrations remained generally low, with two sporadic high - concentration areas observed in the northern and northeastern zones. The highest concentration of cadmium, 0.31 $\mu\text{g L}^{-1}$, was detected at site ZJ12.

The spatial distribution characteristics of heavy metals exhibited a generally consistent trend across the study area, with significantly higher concentrations observed in the eastern and central regions compared to the western zone. This spatial heterogeneity may be attributed to three primary factors: 1) Geological composition differences - The eastern and central areas contain extensive basalt formations where water-rock interactions facilitate heavy metal leaching into groundwater systems, while the western region is dominated by clastic rocks in red bed formations with inherently lower heavy metal content^{16,49}. 2) Anthropogenic influences - The central

Item	As	Cd	Al	Mn	Hg	Co	Cu	Pb	Zn	Ni
Maximum value	5.18	0.31	305.99	57.50	7.05	0.71	3.10	1.22	4.09	1.12
Minimum value	0.09	nd	2.21	0.07	nd	nd	nd	nd	nd	nd
Average value	1.17	0.22	45.44	6.43	0.37	0.10	0.60	0.17	0.49	0.17
Mid-value	0.70	0.23	24.03	1.87	0.00	0.04	0.43	0.00	0.00	0.06
Concentration range	0.09–5.18	nd–0.31	2.21–305.99	0.07–57.50	nd–7.05	nd–0.71	nd–3.10	nd–1.22	nd–4.09	nd–1.12
Standard deviation	1.12	0.08	56.83	11.56	1.19	0.14	0.72	0.31	0.93	0.27
CV%	95.51	35.59	125.06	179.83	321.43	147.45	118.68	178.80	190.45	157.95
Detection rate (%)	100	89.58	100	100	20.83	58.33	72.92	39.58	43.75	93.75
Standard-exceeding ratio (%)	0	0	2.08	0	8.33	0	0	0	0	0
Standard for groundwater quality (GB/T 14848–2017)	10	5	200	100	1	50	1000	10	1000	20
Standards for drinking water quality (GB 5749–2022)	10	5	200	100	1	70	1000	10	1000	20

Table 4. Analysis and statistics of heavy metal concentrations in groundwater in the study area¹/ $\mu\text{g L}^{-1}$. nd indicates no detection detected.

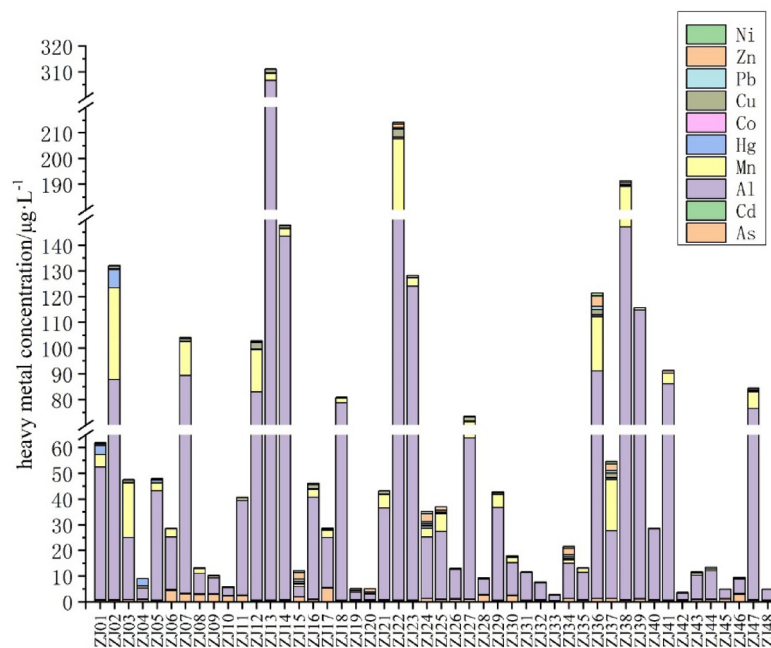


Fig. 2. Accumulation of total concentration of heavy metal elements at sampling point.

region's higher population density and relatively intensive industrial/agricultural activities have exacerbated environmental impacts. Current infrastructure limitations are particularly noteworthy, as only the county seat maintains a centralized wastewater treatment system.³) Pollution pathways - In non-urbanized townships surrounding the central county seat, untreated domestic and industrial effluents are discharged directly into the environment, creating persistent contamination pathways through subsurface infiltration into local aquifers. This multifactorial analysis suggests that both lithogenic processes and anthropogenic pressures collectively shape the observed heavy metal distribution patterns in the study area.

Source analysis of heavy metals

1. Correlation analysis.

The results of Pearson correlation analysis among metallic elements in groundwater samples from the Zhaojue region are presented in Fig. 4. Significant correlations between heavy metal elements may indicate similar sources or analogous migration and transformation processes⁵⁰. The correlation coefficients for heavy metal pairs Zn-Ni, Pb-Ni, and Pb-Zn were 0.92, 0.85, and 0.85 respectively, all passing the correlation test at the 0.01 significance level ($p < 0.01$). This demonstrates statistically significant positive correlations between Zn, Ni, and Pb in pairwise comparisons, suggesting these elements likely share common sources or exhibit similar migration-transformation pathways. For element pairs Cu-Co, Cu-Mn, Mn-Co, and Al-Co, correlation coefficients of 0.83, 0.63, 0.77, and 0.56 were observed respectively (all $p < 0.01$). These moderately strong correlations imply potential partial source overlap or comparable migration-transformation mechanisms among Cu, Mn, Co, and Al. The correlation coefficients between Hg, Cd, As and other elements are all less than 0.4, indicating a weak correlation and suggesting that there may be different sources or migration - transformation processes with certain differences.

2. Principal component analysis.

Principal component analysis is an effective method for identifying the sources of heavy metals^{51,52}. KMO and Bartlett sphericity tests were conducted on the concentration of heavy metals in groundwater in the Zhaojue area in SPSS 26.0, and KMO values (0.730) and Bartlett sphericity test results (0.000) were obtained, indicating that the 10 heavy metals are suitable for principal component analysis. Principal component analysis was conducted on heavy metals in groundwater in the Zhaojue area, and the results are shown in Tables 5 and 6. Three principal components (PCs) were extracted, collectively explaining 77.5% of the total variance. The contribution rates of principal components 1, 2, and 3 were 44.8%, 22.2%, and 10.5%, respectively.

Principal Component 1 (PC1) demonstrated strong loadings for Zn (0.974), Ni (0.928), and Pb (0.908), indicating significant inter-element correlations. These heavy metals are widely recognized as anthropogenic indicators⁵³. Spatial analysis revealed elevated concentrations of Zn, Ni, and Pb predominantly in central and east-central Zhaojue, particularly near population-dense urban centers and major transportation arteries. They

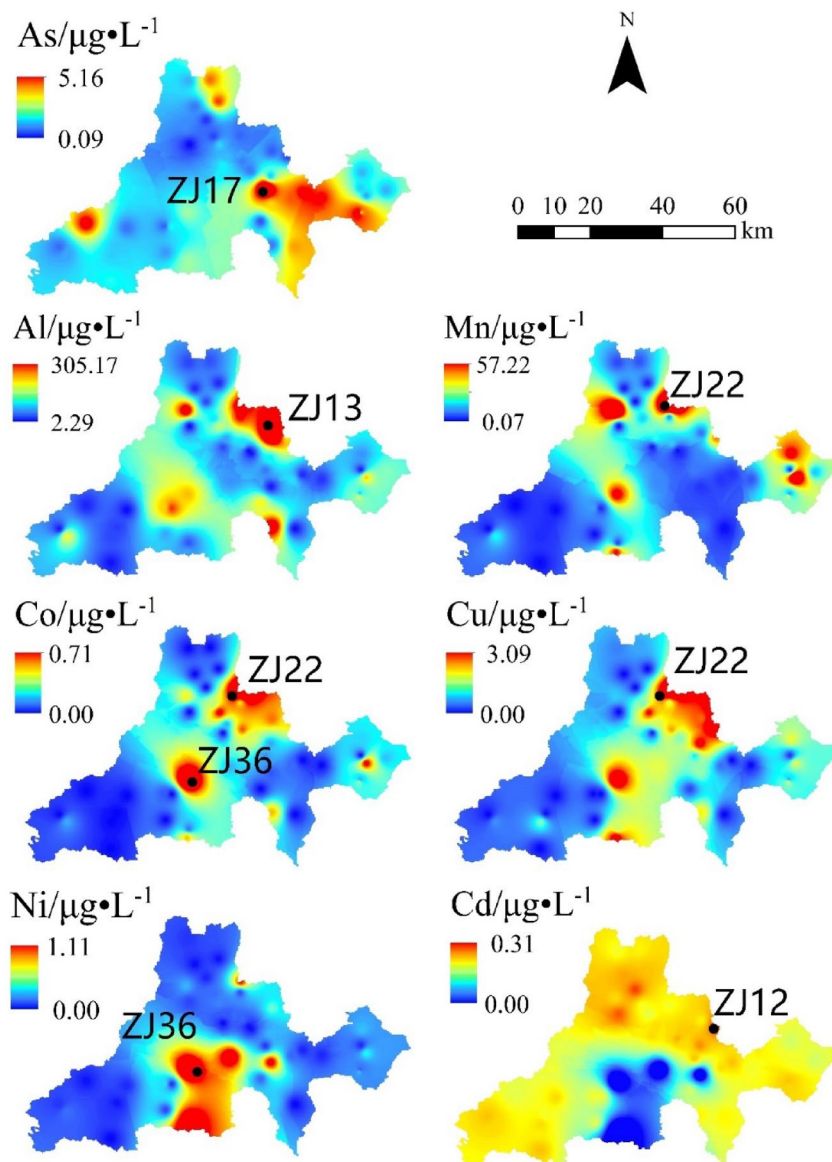


Fig. 3. Spatial distribution of heavy metal from the groundwater.

are areas with frequent human activities and are the main transportation routes for Zhaojue to the outside world. Currently, the lifestyle in the Zhaojue area is relatively traditional, indicating that untreated household waste is directly piled up by the river, and most domestic sewage is directly discharged. Domestic waste and sewage enter the ground under the leaching effect of rainwater, causing pollution to the groundwater in the study area. The heavy metal element Zn may come from household waste⁵⁴. Pb is a landmark element in transportation sources, mainly derived from automobile exhaust and coal combustion^{55,56}, while Ni mainly comes from wastewater generated by industrial pollution^{57,58}. Therefore, it can be considered that PC1 is mainly a human activity factor such as industry, agriculture, and transportation sources.

Principal Component 2 (PC2) exhibited significant loadings for Co (0.888), Cu (0.816), Mn (0.763), and Al (0.762). Spatial clustering of elevated concentrations was observed in central and eastern Zhaojue, corresponding to carbonate formations and Emeishan basalt strata. Notably, Wedepohl⁵⁹ documented elevated Mn concentrations in carbonate rocks, particularly dolostones, with co-occurring Co–Mn associations indicative of lithogenic origins. Geochemical analyses revealed Emeishan basalts in the region contain 10.94–15.22% Al_2O_3 (mean = 13.81%) and exhibit naturally elevated Cu levels, including documented native copper mineralization⁶⁰. These lithological units facilitate elemental mobilization through leaching processes, subsequently enriching groundwater systems. Collectively, PC2 represents a “natural geogenic background factor”, reflecting bedrock weathering dynamics within the regional aquifer system.

The third principal component (PC3) is dominated by Hg, As, and Cd, with Hg exhibiting the highest weight coefficient of 0.961. The elevated Hg concentrations predominantly occur as clustered anomalies in the eastern Zhaojue area, which can be attributed to two main factors: (1) Natural geological processes - the bedrock and soils

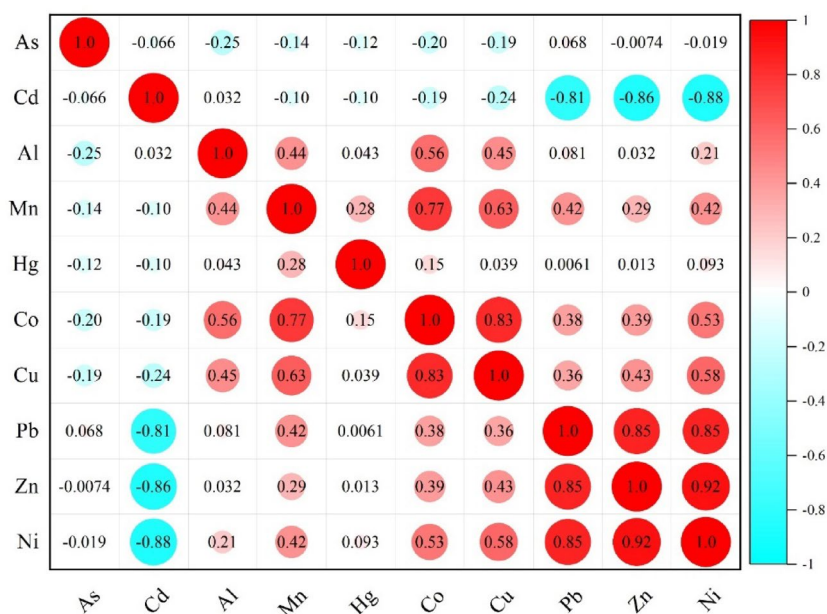


Fig. 4. Correlation coefficient diagram of heavy metal elements in groundwater in the research area.

Component	Initial eigenvalue			Extract square			Rotational sum of squares loading		
	Amount	Variance	Cumulative contribution rate	Total	Variance	Cumulative contribution rate	Total	Variance	Cumulative contribution rate
1	4.48	44.8	44.8	4.48	44.8	44.8	3.74	37.4	37.4
2	2.22	22.2	67.0	2.22	22.2	67.0	2.89	28.9	66.3
3	1.05	10.5	77.5	1.05	10.5	77.5	1.13	11.3	77.5
4	0.91	9.06	86.6	–	–	–	–	–	–
5	0.57	5.67	92.3	–	–	–	–	–	–
6	0.41	4.09	96.4	–	–	–	–	–	–
7	0.14	1.42	97.8	–	–	–	–	–	–
8	0.10	1.01	98.8	–	–	–	–	–	–
9	0.09	0.93	99.7	–	–	–	–	–	–
10	0.03	0.30	100.0	–	–	–	–	–	–

Table 5. Principal component analysis results of heavy metals in groundwater in the research area¹/%. “–” Components with eigenvalues less than 1 have not been extracted and rotated.

Heavy metal elements	PC1	PC2	PC3
Cd	−0.947	0.077	0.348
Zn	0.947	0.137	−0.038
Ni	0.928	0.310	0.016
Pb	0.908	0.171	−0.036
Co	0.274	0.888	0.088
Cu	0.324	0.816	−0.047
Mn	0.232	0.763	0.281
Al	−0.096	0.762	−0.035
As	0.136	−0.342	0.329
Hg	0.058	0.019	0.961

Table 6. Principal component analysis of heavy metal concentration in groundwater in the research area.

	Max	Min	Average value	No pollution	Slightly pollution	Lightly pollution	Moderately polluted	Seriously pollution
As	0.518	0.009	0.117	100	0	0	0	0
Cd	0.0622	0	0.043	100	0	0	0	0
Al	1.53	0.011	0.227	97.92	2.08	0	0	0
Mn	0.575	0.0007	0.064	100	0	0	0	0
Hg	7.046	0	0.369	91.67	2.08	2.08	2.08	2.08
Co	0.0143	0	0.0019	100	0		0	0
Cu	0.0031	0	0.0006	100	0		0	0
Pb	0.1224	0	0.0174	100	0		0	0
Zn	0.0041	0	0.0005	100	0		0	0
Ni	0.0558	0	0.0085	100	0		0	0

Table 7. Single factor pollution index of heavy metals in groundwater in the research area.

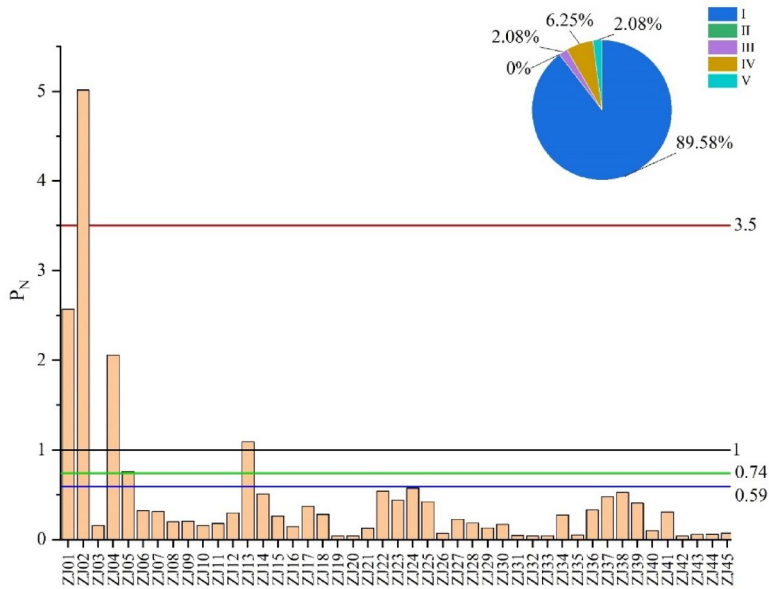


Fig. 5. Nemerow pollution index of heavy metal elements at sampling point.

in this eastern region inherently contain Hg-bearing minerals, which are gradually released into groundwater through long-term physicochemical weathering, erosion, and subsequent leaching/infiltration by atmospheric precipitation⁶; (2) Anthropogenic influences - improper disposal practices such as long-term accumulation of domestic waste and garbage incineration facilitate Hg migration into aquifers through precipitation leaching. Regarding other elements in PC3, As primarily originates from agricultural applications as a key component of insecticides and herbicides⁶¹, while elevated Cd levels result from combined impacts of industrial emissions (waste gas, wastewater, and residues), agrochemical utilization (pesticides and fertilizers), and plastic film residues. These findings collectively demonstrate that PC3 represents a composite signature controlled by both natural geochemical background and anthropogenic activities.

Groundwater quality evaluation

The single-factor pollution index (Pi) of heavy metals in groundwater in the Zhaojue region was assessed according to the Class III of Standard for groundwater quality (GB/T 14848 – 2017). The calculation results are presented in Table 7. The average single-factor pollution index values for As, Cd, Al, Mn, Hg, Co, Cu, Pb, Zn, and Ni are 0.117, 0.043, 0.227, 0.064, 0.369, 0.0019, 0.0006, 0.0174, 0.0005, and 0.0085, respectively. All values are less than 1, indicating that the overall water quality is satisfactory. However, the single-factor exceedance rates for heavy metals Hg and Al are 8.33% and 2.08%, respectively. The maximum single-factor pollution index for Hg (7.046) indicates severe pollution, while the maximum for Al (1.530) indicates mild pollution.

The Nemerow Comprehensive Pollution Index (PN) was used to assess heavy metals in groundwater from sampling sites in Zhaojue, with the results presented in Fig. 5. The PN values for the 48 water samples in Zhaojue range from 0.0355 to 5.014, with an average of 0.4402. Based on the PN values, heavy metal pollution in the water samples can be categorized into five levels. Overall, the quality of heavy metals in the Zhaojue area is good, with 89.58% of samples being free of pollution (Class I), 2.08% mildly polluted (Class III), 6.25% moderately

	Adults			Children		
	Maximum	Minimum	Mean	Maximum	Minimum	Mean
HQing	1.32	0.16	0.73	3.33	0.40	1.83
HQderm	0.01	2.51×10^{-3}	0.01	0.03	2.89×10^{-3}	0.01
HI	1.33	0.16	0.74	3.36	0.41	1.84
CRing	2.47×10^{-4}	4.64×10^{-5}	8.15×10^{-5}	6.21×10^{-4}	1.17×10^{-4}	2.05×10^{-4}
CRderm	4.02×10^{-6}	4.14×10^{-7}	1.10×10^{-6}	3.93×10^{-6}	7.81×10^{-7}	1.37×10^{-6}
ILCR	2.51×10^{-4}	4.69×10^{-5}	8.26×10^{-5}	6.25×10^{-4}	1.17×10^{-4}	2.06×10^{-4}

Table 8. HI and ILCR values for different population groups.

Classification	HMs	Adults		Children	
		Adults	Contribution rate	Children	Contribution rate
Carcinogenic (ILCR)	As	2.28×10^{-3}	57.41%	5.65×10^{-3}	57.12%
	Cd	1.69×10^{-3}	42.54%	4.24×10^{-3}	42.83%
	Pb	1.88×10^{-6}	0.05%	4.72×10^{-6}	0.05%
Non-carcinogenic (HI)	As	5.06	14.33%	12.56	14.19%
	Cd	27.66	78.33%	69.49	78.51%
	Al	4.14×10^{-1}	1.17%	1.04	1.17%
	Co	4.11×10^{-1}	1.16%	1.03	1.16%
	Mn	9.21×10^{-2}	0.26%	1.76×10^{-1}	0.20%
	Pb	6.35×10^{-2}	0.18%	1.59×10^{-1}	0.18%
	Hg	1.58	4.47%	3.98	4.49%
	Cu	1.97×10^{-2}	0.06%	4.88×10^{-2}	0.06%
	Ni	1.09×10^{-2}	0.03%	2.72×10^{-2}	0.03%
	Zn	2.12×10^{-3}	0.01%	5.26×10^{-3}	0.01%

Table 9. The total Non carcinogenic and carcinogenic health risks of different HMs to adults and children.

polluted (Class IV), and 2.08% heavily polluted (Class V). Notably, there is only one Serious pollution point, which is ZJ02, and the exceeding factor is Hg.

Health risk assessment

Based on health risk assessment models and parameters, the non-carcinogenic health risks posed by heavy metals in groundwater through drinking water ingestion and dermal exposure pathways were quantified, as presented in Table 8.

The ranges of HQ_{ing} for adults and children are from 0.16 to 1.32 (mean:0.73) and from 0.40 to 3.33 (mean: 1.83), respectively. The ranges of HQ_{derm} for adults and children are from 2.51×10^{-3} to 0.01 (mean: 0.01) and from 2.89×10^{-3} to 0.03 (mean: 0.01), respectively. In addition, the ranges of HI for adults and children are from 0.16 to 1.33 (mean: 0.74) and from 0.41 to 3.36 (mean: 1.84), respectively. For adults, the HI values of three samples are greater than 1, indicating non-carcinogenic risks, while the HI values of the other samples are within the acceptable level. For children, HI values for only four samples were below 1 (indicating no non-carcinogenic risk), while those for the remaining forty-four samples exceeded 1 (indicating non-carcinogenic risks). The study also shows that the HI values of children are higher than those of adults, suggesting that children are at a greater risk. The average value of HQ_{ing} for children is approximately twice that for adults, while the average values of HQ_{derm} are both 0.01. Therefore, the non-carcinogenic risks of heavy metal elements are mainly associated with the ingestion of drinking water.

According to the results, the range of CR_{ing} for adults is between 4.64×10^{-5} and 2.47×10^{-4} (mean: 8.15×10^{-5}), while the range of CR_{derm} is between 4.14×10^{-7} and 4.02×10^{-6} (mean: 1.10×10^{-6}). The range of CR_{ing} for children is from 1.17×10^{-4} to 6.21×10^{-4} (mean: 2.05×10^{-4}), and the range of CR_{derm} is from 7.81×10^{-7} to 3.93×10^{-6} (mean: 1.37×10^{-6}). These results indicate that the drinking water ingestion pathway is the main exposure pathway.

The ILCR values for adults and children are in the ranges of 4.69×10^{-5} to 2.51×10^{-4} (mean: 8.26×10^{-5}) and 1.17×10^{-4} to 6.25×10^{-4} (mean: 2.06×10^{-4}), respectively. For adults, the ILCR values of 10 samples are higher than the threshold value of 1.0×10^{-4} , accounting for 20.8%. For children, the ILCR values of all samples are higher than the threshold value of 1.0×10^{-4} . This implies that the groundwater in the surveyed area poses a considerable carcinogenic risk, and the carcinogenic risk of groundwater pollutants to children is even higher.

The total non-carcinogenic and carcinogenic health risks of different heavy metals (HMs) are presented in Table 9 for adults and children, respectively. As illustrated in Table 9, the non-carcinogenic contribution order of pollutants to adults and children was Cd > As > Hg > Al > Co > Mn > Pb > Cu > Ni > Zn. Obviously, Cd was the major contaminant, accounting for 78.33% and 78.51% of the total HI for adults and children, respectively.

As shown in Table 9, As accounted for 57.41%, while Cd and Pb accounted for 42.54% and 0.05% of the total carcinogenic risk for adults, respectively. Similar results were obtained considering health risk assessment for children. These results show that As contributes the most to carcinogenic risk, indicating that arsenic is the major contaminant.

Conclusion

This study systematically assesses heavy metal contamination in the groundwater of the Zhaojue area, Sichuan Province, by integrating pollution indices, spatial analysis, source apportionment, and health risk models. The findings are as follows:

1. The order of the average concentrations of metal elements in the study area is as follows: $Al > Mn > As > Cu > Zn > Hg > Cd > Pb > Ni > Co$. According to the groundwater quality standards and drinking water standards, the concentration of Al at one sampling point in the study area exceeds the standard value, and the concentrations of Hg at three sampling points exceed the standard limits, which should be the key points of future prevention and control work of heavy metal pollution in groundwater.
2. The overall trends of the spatial distribution characteristics of different heavy metals are consistent, that is, the concentrations of heavy metals in the eastern and central regions are higher than those in the western region.
3. The results of source apportionment indicate that the heavy metals Zn, Ni, and Pb in the water bodies of the study area originate from industrial, agricultural, and transportation sources. Co, Cu, Mn, and Al mainly come from the geological background, while Hg, As, and Cd are jointly controlled by the natural geological background and human activities.
4. The single-factor evaluation shows that the heavy metal elements Hg and Al exceed the clean level. The evaluation by the Nemerow comprehensive pollution index method indicates that the overall quality of groundwater in the Zhaojue area is good, and the proportion of non-polluted water (Class I) accounts for 89.58%.
5. The health risk assessment revealed notable disparities between adults and children regarding heavy metal exposure in groundwater. For non-carcinogenic risks, children exhibited higher hazard indices (HI: 0.41–3.36) than adults (HI: 0.16–1.33), with forty-four samples exceeding safe thresholds (HI > 1). Carcinogenic risks further highlighted vulnerability, as all child samples exceeded the incremental lifetime cancer risk (ILCR) threshold (1.0×10^{-4}), compared to 20.8% of adult samples. Arsenic was the main pollutant and ingestion was the main exposure pathway. These findings underscore significant carcinogenic risks in the surveyed area, particularly for children, emphasizing the critical need for targeted groundwater management to mitigate ingestion-related health threats.

Data availability

All data generated or analysed during this study are included in this published article.

Received: 8 January 2025; Accepted: 25 July 2025

Published online: 28 August 2025

References

1. Li, X., Li, Y., Wang, J., Zhang, X. & World Water, U. N. Development report 2022 pays attention to ground water protection and management. *World Environ.* **02**, 44–46 (2023) (in Chinese).
2. Wang, X., Sato, T., Xing, B. & Tao, S. Health risks of heavy metals to the general public in tianjin, China via consumption of vegetables and fish. *Sci. Total. Environ.* **350**, 28–37 (2005).
3. Joseph, P. Mechanisms of cadmium carcinogenesis. *Toxicol. Appl. Pharmacol.* **238**, 272–279 (2009).
4. Monika, M. et al. A comprehensive study on aquatic chemistry, health risk and remediation techniques of cadmium in groundwater. *Sci. Total. Environ.* **818**, 151784 (2022).
5. Kim, K.-H., Kabir, E. & Jahan, S. A. A review on the distribution of hg in the environment and its human health impacts. *J. Hazard. Mater.* **306**, 376–385 (2016).
6. Gao, R. et al. Health risk assessment of Cr6 +, as and hg in groundwater of Jilantai salt lake basin, China. *China Environ. Sci.* **38**, 2353–2362 (2018) (in Chinese).
7. Imran, W. & Richardson, J. B. Trace element (As, cd, cr, cu, pb, se, U) concentrations and health hazards from drinking water and market rice across Lahore City, Pakistan. *Sustainability* **15**, 13463 (2023).
8. Hajahmadi, Z., Younesi, H., Bahramifar, N., Khakpour, H. & Pirzadeh, K. Multicomponent isotherm for biosorption of Zn(II), CO(II) and Cd(II) from ternary mixture onto pretreated dried *Aspergillus Niger* biomass. *Water Resour. Ind.* **11**, 71–80 (2015).
9. Li, S., Shi, X., Qian, H. & Xu, P. Applicability analysis of different evaluation methods in groundwater quality evaluation: A case of Xi'an city. *IOP Conf. Ser. Earth Environ. Sci.* (2023).
10. Su, K., Wang, Q., Li, L., Cao, R. & Xi, Y. Water quality assessment of Lugu lake based on Nemerow pollution index method. *Sci. Rep.* **12**, 13613 (2022).
11. Elemile, O. O., Ibitogbe, E. M., Folorunso, O. P., Ejiboye, P. O. & Adewumi, J. R. Principal component analysis of groundwater sources pollution in Omu-Aran community, Nigeria. *Environ. Earth Sci.* **80**, 690 (2021).
12. Boschetti, T. et al. Using principal component analysis to distinguish sources of radioactivity and nitrates contamination in Southern Tunisian groundwater samples. *J. Geochem. Explor.* **271**, 107670 (2025).
13. Fan, H., Zhou, Q., Xu, X. & Yao, Y. Characterization of spatial and temporal distribution of arsenic concentration in groundwater in China and its health risk assessment. *Environ. Ecol.* **6**, 1–14 (2024).
14. Tokatli, C., Mutlu, E., Ustaoglu, F., Islam, A. R. T. & Muhammad, S. Spatiotemporal variations, health risk assessment, and sources of potentially toxic elements in Potamic water of the Anday stream basin (Türkiye), black sea region. *Environ. Monit. Assess.* **196**, 420 (2024).
15. Zhou, C., Li, J., Zou, S. & Lin, Y. Study on geological survey + economic development model in Wumeng Mountainous area: A case study of Zhaojue County. *Geol. Surv. China* **10**, 120–130 (2023).
16. Cao, J., Liu, M., Shen, H., Zheng, X. & Yang, L. Geochemical characteristics of the Emeishan Basalt in Zhaojue area, Sichuan province. *Acta Geologica Sichuan* **43**, 512–519 (2023) (in Chinese).

17. Zhou, C., Zou, S., Zhu, D. & Lin, Y. Characteristics, causes and development suggestions of high quality metasilicate groundwater in Zhaojue area, Sichuan Province. *Geol. China* **49**, 849–859 (2022) (in Chinese).
18. Fan, L. et al. Unique characteristics of groundwater occurrence and its development and utilization model in the Wumeng mountain area—a case study of the Zhaojue area. *Acta Geol. Sinica* **95**, 3544–3555 (2021) (in Chinese).
19. Lu, L. et al. Hydrogeochemical characteristics and genesis of Zhuhe hot springs in zhaojue, Sichuan Province. *Geoscience* **35**, 703–710 (2021) (in Chinese).
20. Lin, Y., Zou, S., Wang, J. & Li, J. Hrdrochemical characteristics and water quality assessment of Emei mountain basalt groundwater. *Yangtze River* **52**, 20–24+48 (2021) (in Chinese).
21. Zuo, C., Xu, Q., Yang, X., Surveys and analysis of geological disasters in Zhaojue County of Sichuan. *Res. Soil Water Conserv.*, 177–179+183 (2008) (in Chinese).
22. Wang, W., Gao, P., Li, J. & Zhou, Y. Water quality assessment and trend analysis of typical tributaries of Danjiangkou Rservoir. *Water Resour. Prot.* **32**, 127–130 (2016) (in Chinese).
23. Chai, L. et al. Pollution characteristics, spatial distributions, and source apportionment of heavy metals in cultivated soil in Lanzhou, China. *Ecol. Indic.* **125**, 107507 (2021).
24. Zhang, J., Wu, L. & Feng, X. Application and research of Nemerow comprehensive index method in heavy metal pollution assessment of river sediment. *Ground Water* **45**, 113–116 (2023) (in Chinese).
25. Li, S., Xiong, J., Deng, C. & Wang, X. Heavy metal pollution status and health risk assessment of Liujiang water in the Xijiang river basin. *Guangxi Sci.* **25**, 393–399 (2018) (in Chinese).
26. Giri, S. & Singh, A. K. Risk assessment, statistical source identification and seasonal fluctuation of dissolved metals in the Subarnarekha river, India. *J. Hazard. Mater.* **265**, 305–314 (2014).
27. Wang, J., Liu, Z., Gu, X. & Gao, Z. Health risk assessment methods for environmental carcinogens. *J. Environ. Hyg.* **36**, 50–58 (2009) (in Chinese).
28. USEPA. Risk assessment guidance for superfund Volume I: Human health evaluation manual. Supplemental Guidance: Standard default exposure factors final interim report (Directive). (US EPA, 1991).
29. USEPA. Guidelines for exposure assessment (Office of Health and Environmental Assessment US EPA, 1992).
30. USEPA. Risk assessment guidance for superfund Volume I: human health evaluation manual (Part F, supplemental guidance for inhalation risk assessment). (U. S. Environmental Protection Agency, 2009).
31. Vesković, J., Milić, A., Lučić, M. & Onjia, A. Appraisal of contamination, hydrogeochemistry, and Monte Carlo simulation of health risks of groundwater in a lithium-rich ore area. *Environ. Geochem. Health* **46**, 468 (2024).
32. Yuan, Y., Liu, Y., Luo, K. & Shahid, M. Z. Hydrochemical characteristics and a health risk assessment of the use of river water and groundwater as drinking sources in a rural area in Jiangjin district, China. *Environ. Earth Sci.* **79**, 160 (2020).
33. Zhou, J. et al. Distribution and health risk assessment of metals in groundwater around iron mine. *China Environ. Sci.* **39**, 1934–1944 (2019) (in Chinese).
34. Duan, X. *Highlights of the Chinese Exposure Factors Handbook (Children)* (China Environmental Science Press, 2016).
35. Fu, R., Xin, C., Yu, S. & Li, X. Analysis of heavy metal sources in groundwater and assessment of health risks: an example from the Southwest Sub-basin of the Shiqi river. *Environ. Sci.* **44**, 796–806 (2023) (in Chinese).
36. Duan, X. *Highlights of the Chinese Exposure Factors Handbook (Adults)* (China Environmental Science Press, 2014) (in Chinese).
37. Qiao, J. et al. Distributions of arsenic and other heavy metals, and health risk assessments for groundwater in the Guanzhong plain region of China. *Environ. Res.* **181**, 108957 (2020).
38. Xie, H. et al. Spatial distribution, source analysis, and health risk assessment of metal elements in karst water in southeastern Chongqing. *Environ. Sci.* **44**, 4304–4313 (2023) (in Chinese).
39. USEPA. Superfund public health evaluation manual. (US EPA, 1986).
40. Shu, L. et al. Analysis on variation of groundwater flow field and its main influencing factors in the typical district of Sanjiang plain. *J. Hydraul. Eng.* **53**, 644–654 (2022) (in Chinese).
41. Egbueri, J. C. Heavy metals pollution source identification and probabilistic health risk assessment of shallow groundwater in onitsha, Nigeria. *Anal. Lett.* **53**, 1620–1638 (2020).
42. Liu, W., Gao, Z., Xu, Y. & Han, C. Hydrochemical characteristics and water quality evaluation of karst water in Jinan City. *Carsologica Sinica* **42**, 220–232 + 244 (2023) (in Chinese).
43. Shang, T., Zhang, Y., Zhou, J., Ding, J. & Zhang, Z. Application of multivariate statistical analysis in the analysis of heavy metal pollution sources in farmland soil. *Environ. Ecol.* **4**, 93–97 (2022) (in Chinese).
44. Bodrud-Doza, M. et al. Characterization of groundwater quality using water evaluation indices, multivariate statistics and geostatistics in central Bangladesh. *Water Sci.* **30**, 19–40 (2016).
45. Mackiewicz, A. & Ratajczak, W. Principal components analysis (PCA). *Comput. Geosci.* **19**, 303–342 (1993).
46. Wang, F., Jiqin, K., Cao, J. & Wang, R. Source characteristics and influencing factors of groundwater hydrochemistry in the karst areas of central Guizhou. *Carsologica Sinica* **43**, 889–899 (2024) (in Chinese).
47. Stoeva, N., Berova, M. & Zlatev, Z. Effect of arsenic on some physiological parameters in bean plants. *Biol. Plant.* **49**, 293–296 (2005).
48. Shi, H. et al. Source analysis and health risk assessment of heavy metals in groundwater of Leizhou Peninsula. *Environ. Sci.* **42**, 4246–4256 (2021).
49. Zhao, C. et al. Geochemical characteristics of selenium in surface soil of central townships in Zhaojue county, Sichuan Province. *Rock Miner. Anal.* **41**, 412–426 (2022) (in Chinese).
50. Zhang, Y., Guo, C., Sun, Pa. & Zhu, Y. Groundwater health risk assessment based on spatial analysis in the Qiaomaidi watershed. *China Environ. Sci.* **39**, 4762–4768 (2019).
51. Zhang, J. et al. Pollution characteristics and risk assessment of heavy metals in water and sediment from Daye lake. *Environ. Sci.* **38**, 2355–2363 (2017) (in Chinese).
52. Lv, J. et al. Analysis of soil heavy metal sources and environmental risk assessment in Rizhao City. *Acta Geogr. Sin.* **67**, 971–984 (2012) (in Chinese).
53. Pu, Y., Tu, Y., You, Z., Duan, Y. & Cao, S. Pb–Zn isotopic tracing technique in sediments: review and propectives. *Environ. Chem.* **36**, 581–590 (2017) (in Chinese).
54. Li, J. et al. Chemical analysis and evaluation of heavy metal pollution in sewage sludge and its leachate. *J. Saf. Environ.* **13**, 115–121 (2013) (in Chinese).
55. Cai, L., Ma, J., Zhou, Y., Huang, L., Dou, L., Zhang, C. & Fu, S., Multivariate geostatistics and GIS-based approach to study the Spatial distribution and sources of heavy metals in agricultural soil in the Pearl river delta, China. *Environ. Sci.*, 3496–3502 (2008) (in Chinese).
56. He, S., Zhao, R., Li, Z., Huang, S. & Lai, X. Health risk assessment and source analysis of heavy metals in the Liangtan river basin of Chongqing City. *J. Hydroecol.* **44**, 115–123 (2023) (in Chinese).
57. Yang, Y., Liu, L. & Chen, M. Characteristics and source analysis of heavy metal pollution in surface soil of Nanjing City in the Yangtze river delta region. *China Environ. Sci.* **44**, 3910–3918 (2024) (in Chinese).
58. Lv, J. et al. Identifying the origins and Spatial distributions of heavy metals in soils of Ju country (Eastern China) using multivariate and Geostatistical approach. *J. Soils Sediments* **15**, 163–178 (2015).
59. Wedepohl, K. H. *Handbook of Geochemistry: v.2/5B* (Springer, 1978).

60. Li, J. *Geochemical Study on Permian Emeishan Flood Basalts in Zhaotong Area, Yunnan Province, SW China*. thesis, (The University of Chinese Academy of Sciences, 2016) (in Chinese).
61. Chen, T. et al. Identification of trace element sources and associated risk assessment in vegetable soils of the urban–rural transitional area of Hangzhou, China. *Environ. Pollut.* **151**, 67–78 (2008).

Acknowledgements

The work was supported by Project Supported by the China Geological Survey Project (DD202305007, DD20190825 and DD20230081), and Guangxi Science and Technology Planning Project (GuiKe AD21196001).

Author contributions

Study conception and design: Y.L., Methodology: Y. L., J. L. and S. Z., Sample collection and formal analysis: Y. L., J. L., S. Z., J. W., L. F., C. Z. and L. L.. Writing – original draft: Y. L., J. L. and S. Z., Writing – review & editing: Y. L., J. L., S. Z., J. W., L. F., C. Z., L. L. Project administration: S. Z. All authors read and approved the final manuscript.

Declarations

Competing interests

The authors declare no competing interests.

Additional information

Correspondence and requests for materials should be addressed to Y.L.

Reprints and permissions information is available at www.nature.com/reprints.

Publisher's note Springer Nature remains neutral with regard to jurisdictional claims in published maps and institutional affiliations.

Open Access This article is licensed under a Creative Commons Attribution-NonCommercial-NoDerivatives 4.0 International License, which permits any non-commercial use, sharing, distribution and reproduction in any medium or format, as long as you give appropriate credit to the original author(s) and the source, provide a link to the Creative Commons licence, and indicate if you modified the licensed material. You do not have permission under this licence to share adapted material derived from this article or parts of it. The images or other third party material in this article are included in the article's Creative Commons licence, unless indicated otherwise in a credit line to the material. If material is not included in the article's Creative Commons licence and your intended use is not permitted by statutory regulation or exceeds the permitted use, you will need to obtain permission directly from the copyright holder. To view a copy of this licence, visit <http://creativecommons.org/licenses/by-nc-nd/4.0/>.

© The Author(s) 2025